ORIGINAL RESEARCH

Role of Perfusion MRI and 1H Spectroscopy in the Evaluation of Brain Tumors- a Study in the Asian Subpopulation

Shaafiya Ashraf[1], Adnan Zahoor[2], Mihir Munshi[3], Sudarshan Aggarwal[3]

ABSTRACT

Introduction: The role of MR Perfusion and 1H Spectroscopy in the evaluation of brain tumors has been extensively studied. We attempt to validate the same in the Asian sub population.

Materials and Methods: 25 cases of primary and 2 secondary brain tumors were evaluated; 17 pretreatment and 11 post treatment. Routine pre and post contrast sequences, dynamic susceptibility weighted perfusion and CSI or SVS spectroscopy was performed

Results: All viable tumors showed elevated rCBV, N-Cho, Cho/Cr &Cho/ NAA and decreased N-NAA. Sensitivity of Cho/NAA was lower compared to the N-Cho. Peritumoral rCBV and altered spectra helped determine true tumor extent. Contrast T1WI allowed grading in only 60% cases of solid gliomas whereas with rCBV it was possible in all cases. rCBV increased progressively from grade II to IV. Grade IV gliomas had lower Cho level than grade IIIs and had elevated lipids. Rim enhancing necrotic tumors had high Cho, NAA, Cho /NAA & Cho/Cr, a lactate and a lipid peak. Metastasis showed characteristic perfusion mean curve (recovery phase) and no /absent NAA. Both viable tumor and post treatment changes showed post contrast enhancement however elevated rCBV, Cho, Cho/NAA, Cho/Cr was seen in viable tumor tissue where as low rCBV, NAA, Cho& Cr and elevated lipid- lactate was seen in post treatment necrosis.

Conclusion: Perfusion MRI and spectroscopy allowed preoperative identification and grading of brain tumors, characterization as primary intraaxial or metastatic tumor as well as distinction of viable tumor tissue from post treatment changes.

Keywords: Brain Tumor grading, Perfusion MRI, Spectroscopy

How to cite this article: Shaafiya Ashraf, Adnan Zahoor, Mihir Munshi, Sudarshan Aggarwal. Role of Perfusion MRI and 1H Spectroscopy in the Evaluation of Brain Tumors- a Study in the Asian Subpopulation. International Journal of Contemporary Medical Research 2015;2(5):1159-1165.

[1]Lecturer in Department of Radiodiagnosis, [2]Registrar in Department of Orthopaedics, Government Medical College, Srinagar, Jammu and Kashmir, [3]Consultant, Diwan Chand Satyapal Aggarwal Imaging Centre, New Delhi, India.

Corresponding author: Dr Shaafiya Ashraf D.N.B., Lecturer Department of Radiodiagnosis, Government Medical College Srinagar, Jammu and Kashmir, India

Source of Support: Nil

Conflict of Interest: None

INTRODUCTION

The physiology and anatomy of the brain, sets apart the behavior of tumor cells as well as the goals of brain tumor imaging. The critical factors in evaluating prognosis are[1,2,3,] confirmation of the tumor presence, type, anatomical details of site, number and spatial extent, grading of tumors and differentiation of post treatment changes from viable tumor.

Conventional MR has high sensitivity with excellent anatomical delineation. However it relies heavily on contrast enhancement, which is largely inadequate in[4,5] distinguishing between tumor, edema and nonspecific treatment effects in the region of T2 hyperintensity as well as for tumor grading. Perfusion MRI and Proton MR spectroscopy have helped overcome these problems by exploiting changes in hemodynamics, proton motion and metabolic activity within the tumor. Perfusion calibrates the tumor hypoxia induced neovascularity i.e. CBV, CBF and MTT normalized to the contralateral white matter. CBF and MTT have not been found detrimental for oncologic imaging. MR spectroscopy using the concept of chemical shift performs biochemical analysis in vivo to determine concentration of metabolites within tissues[6-11] Several studies have been conducted to demonstrate their application in oncologic imaging. Our study aimed at validating the same in the patient profile in the Asian subcontinent.

MATERIALS AND METHODS

The study was conducted at Diwan Chand Aggarwal Imaging Research Centre New Delhi

Patient selection and sample size

25 cases of primary and 2 secondary brain tumors were included in the study. 17 patients were evaluated pretreatment and 8 post treatment after getting proper informed consent for the said study. However, no ethical committee approval is required as not being a therapeutic study.

Methodology

MRI was performed on a 1.5 Tesla Seimens Magnetom AVANTO scanner.

Non contrast: Axial spin echo T1, TSE T2, FLAIR and DWI. Sagittal and coronal T2WI.

Contrast
Echo planar dynamic T2* susceptibility weighted perfusion imaging using endogenous tracer technique and post contrast axial, coronal and Sagittal T1 weighted images.
MRS-CSI multivoxel with TE 135ms and if required TE 30ms and TE 270ms or SVS 30ms.

Technique
Perfusion MRI
13 slices were acquired every 1500 msec over 120 sec, for a total of 60 image sets (780 images). TR, 1500 msec; TE, 90 msec; slice thickness 5mm,matrix size, 128 x 128; and field of view, 24 x 24 cm. After the first 15 image sets were obtained, a 0.2-mmol/kg bolus of gadopentetate dimeglumine was power-injected via an 18- or 20-gauge IV catheter at a rate of 4 ml/sec, to allow for a tight bolus of contrast material. Successive images where then acquired during the first pass of contrast material through the brain. The imaging planes through the tumor were chosen to contain a major intracranial artery feeding the neoplasm (typically the ipsilateral paraclinoid internal carotid artery or middle cerebral artery). rCBV maps were generated. Arterial input function was obtained by manually selecting a small population of voxels that satisfied the criteria of being characteristic for arteries i.e. early arrival time, large peak and a short mean transit time. The maps were generated by numeric integration from beginning to end of the first-pass transit of a bolus of contrast agent using constant baseline signal intensity.
H1 MR Spectroscopy
Multivoxel 2D proton CSI was performed in most patients. However in some, SVS was performed depending on the lesion location or time constraint. A volume selective 2D proton CSI sequence with 1500/144 was used. The hybrid multivoxel CSI technique used point-resolved spectroscopy (PRESS) double spin-echo sequence for preselection of a VOI to include the abnormality as well as normal-appearing brain tissue when possible. A 16 x 16 phase-encoding matrix was used to obtain the 8 x 8 array of spectra in the VOI, with an in-plane resolution of 1 x 1 cm and a voxel size of 1 x 1 x 1.5 cm^3 or 1 x 1 x 2 cm^3. Partial volume averaging was prevented by minimizing the mixing of gray and white matter, avoiding CSF, positioning away from scalp(to reduce the contamination with lipids), sinuses, bones and blood vessels and placing saturation bands at the edges of the CSI matrix grid.

Acquisition parameters
TR 1500ms, TE 30ms, 135ms and/270ms, number of acquisitions 128-256 and TA of 7-8 min.

Reconstruction and Post processing of 1-H MRSI Data
Maximal Cho, Cr, Cho/Cr and Cho/NAA ratios and minimum NAA and NAA/Cr ratios were obtained from spectral maps. Other peaks detected included lactate, lipids, alanine and myoinositol. To calculate normalized ratios (N-Cho, N-NAA and N-Cr) values were obtained in normal-appearing white matter in the contralateral hemisphere. Analysis of the frequency spectra was done for peak height, area, shape and multiplicity of the peaks.

RESULTS

25 cases were studied (table 1), male female ratio of 4:1 and age range of 35- 60yrs
14 patients presented pre biopsy. Histopathologic correlation was obtained post operatively in 12. 2 patients with LGG were followed with subsequent MRIs.
3 patients had underwent biopsy or recent debulking. 11 patients presented post op /post treatment for follow up studies. Of these, one patient with recurrence underwent subsequent histopathological evaluation. The findings of the remaining 10 were correlated with clinical data and validated with followup MR and / PET studies. The rCBV maps and MR spectra from the lesions were of analyzable quality in all patients. All viable tumors showed rCBV higher than the contralateral normal white matter ranging from 1-21. All tumor spectra differed from the spectra of normal brain tissue. The differences exceeded the variances caused by the differences in patient age or tumor location, which contributes to the variances of the control spectra.
The most common intra axial lesions were gliomas - astrocytoma subtype. 18 of our patients were astrocytomas (72%). The rCBV values and metabolite distribution pattern of the astrocytomas corresponded with the tumor grade.

Grade I-II LGGs (table 2)
None of these showed contrast enhancement. Myoinositol

	Frequency	Percent
LGG- Fibrillary astrocytoma (patient 4,23,24)	3	12.0
HGG SOLID - Anaplastic astrocytoma -5, GBM-11	13	52.0
NECROTIC HGG -GBM (patient 2,5)	2	8.0
OLOGODENDROGLIOMAS (patient.1,3)	2	8.0
METASTATSIS(patient 22,25)	2	8.0
Total	25	100.0

Table-1: Frequency Table

Parameter	Range	Mean
rCBV	1.1 1.6	1.3± 0.27
N – Choline	1.3 – 1.45	1.3 ± 0.08
N – NAA	0.1 – 0.55	0.36 ± 0.2
N – Cr	0 – 1	0.51 ± 0.15
Cho/NAA	1.5 – 9.5	4.2 ± 0.45
Cho/Cr	1 – 2	1.4 ± 0.45
Lipid	Absent	
Lactate	2 patients	

Table-2: Grade II gliomas

was seen in 1 case. One patient was operated and found to have a fibrillary astrocytoma. Two patients were not operated however the lesion size and morphology was stable on subsequent MRIs indicating that these were also low grade gliomas.

Grade III astrocytomas

(anaplastic astrocytomas) **(**table 3**)**. All cases showed contrast enhancement.

The tumors showed internal heterogeneity. The areas of high perfusion corresponded with areas of maximal choline elevation or NAA depression suggesting that these represented regions of higher grade within the same tumor.

Grade IV gliomas (table 4)

GBMs-were 10 in number. 4 patients presented pre treatment and 5 presented with post treatment recurrence. 2 had predominantly necrotic lesions (table 5).

14 lesions showed enhancement and 1 (patient 4) did not show enhancement. When compared the differences in the rCBV and Cho, Cho/Cr & Cho/NAA ratios between LGGs and HGGs were statistically significant and consistent with a threshold value of 1.7 for rCBV and 1.3 for N- Cho. The Cho/NAA ratio although conformed to a threshold value of 1.6 in most cases however there was some overlap among the two groups with one patient with fibrillary astrocytoma having a Cho/NAA of 9.5.

Two cases of oligodendrogliomas were seen with the classical frontal lobe location and calcification on the susceptibility weighted images. Perfusion was high with rCBV values 4.7 – 5.9 (mean 5.7 ±0.8), N-Cho 1.72 – 3.8(mean 2.7 ±1.4), N-NAA 0.16 – 0.33 (mean 0.2 ±.1), N-creatine1.0 – 1.0(mean 0.8 ±0.2), Cho/NAA 1.02 – 3.9(mean 2.8 ±0.14), Cho/Cr 0.9 – 1.6(mean 1.2 ± 0.4). One had elevated lipids and no lactate and the second had elevated lactate without lipids.

Parameter	Range	Mean
rCBV	1 – 15.1	7.19± 4
N – Choline	1.3 – 3.8	2.5 ±.94
N – NAA	0.12 –.75	.29 ±.26
N – Cr	0 – 3	1.03± 1
Cho/NAA	1.5 – 9.5	4.2±4.5
Cho/Cr	1.3 – 3.3	2.1±1
Lipid	6 patients	
Lactate	7 patients	

Table-3: Grade III astrocytomas

Parameter	Range	Mean
rCBV	3.5 – 19.4	9.9 ± 5
N – Choline	0.9 – 2.4	1.5 ±.53
N – NAA	0 – 1.0	0.69 ±0.3
N – Cr	0.07 – 0.46	0.29 ±.14
Cho/NAA	1.5 – 6.7	3.5 ± 1.4
Cho/Cr	0.9 – 2.0	1.2 ± 0.4

Table-4: Solid grade IV gliomas

Parameter	Range	Mean
rCBV	6.1- 8.5	7.2 ±1.6.
N – Choline	1.1	1.1
N – NAA	0.16 – 0.38	0.27 ± 0.15
N – Cr	0 – 1	0.49 ± 0.26
Cho/NAA	1.7 – 3.9	3.8 ±1.4
Cho/Cr	1.2 – 1.6	1.4 ±0.25
Lipid	Both cases	
Lactate	Both cases	

Table-5: Predominantly necrotic high grade (IV) gliomas

Metastasis

Two cases were included in the study: primary bronchogenic carcinoma and endometrial carcinoma. Very high rCBV 10.6- 11.3 (mean 10.9), rCBV, elevated Choline N-Cho 1.43-4.43(mean 3.0) and reduced Cr N-Cr 0.76-1.28 (mean 0.34) was seen. Low levels of NAA were detected in the lesions probably due to partial volume averaging from normal brain parenchyma or voxel contamination. Cho/NAA 3.3-35(mean 19.1) and Cho/Cr 1.8-9.35(mean 5.5).No detectable lactate, but a strong lipid peak was seen in both lesions.

11 patients presented post treatment- post op &/chemo-radiotherapy. 8 were grade IV gliomas, 2 grade III anaplastic astrocytomas and 1 oligodendroglioma on previous histopathology. All had areas of signal abnormality on conventional MRI which needed to be categorized as residual/ recurrent tissue or benign post treatment changes. However only seven showed elevated rCBV ratios and elevated Cho, Cho/NAA and Cho/Cr suggestive of them being residual or recurrent lesions. Of these, one patient underwent debulking which was grade IV GBM with oligodendroglial differentiation on histopathology. In the other six the findings correlated with clinical data, follow up MR /PET CT evaluation. Patient 14 showed rCBV values lower than the contralateral white matter. Also seen were flattened peaks with depressed NAA, Cho, and Cr. An intense peak consistent with lactate and lipids was seen between 0-2 ppm indicative of cellular break down products seen in radiation necrosis called the death peak. This finding was further substantiated by followup PET study which showed no metabolic activity.

DISCUSSION

Conventional contrast MRI has limited ability to evaluate brain tumors i.e true tumor size, differentiation of high grade from low grade tumors and distinction of post treatment changes from proliferating neoplasms. For these reasons, the role of functional MR imaging such as perfusion weighted imaging and MR spectroscopy has been extensively investigated. Our study aimed at evaluating the same in the Indian subpopulation.

A. Identification of tumors

Conventional MRI contrast enhancement depends on disrup-

tion of BBB therefore a tumor with maintained BBB may be nonenhancing or non neoplastic lesions that enhance may look like tumors. In our study conventional MRI was able to accurately characterize the lesions in only 56% of the subjects. Non enhancing tumors, necrotic tumors & post operative changes posing diagnostic dilemmas. However all histological proven viable tumors had elevated rCBV values ranging from 1-21 suggesting a 100% sensitivity. Radiation necrosis which showed nonspecific enhancement had low rCBV. What was most significant about these results was that no lesion with exclusively high rCBV foci proved to be non neoplastic (no false positives) and vice versa. Maximum peritumoural rCBV high grade gliomas was elevated and it preceded the appearance of contrast enhancement suggesting that it can estimate the actual tumor size beyond the margins of enhancement. Spectroscopy consistently revealed reduced or absent NAA, increased choline, lactate and in some lesions lipids (table 2 to 4). Several studies[12,13,14] validate the importance of Cho/NAA and Cho/Cr values as well as N-Cho ratio for detection of tumor. In our study all primary brain tumors showed elevation of Cho/NAA ratio. However radiation necrosis also showed elevated Cho/NAA. Conversely the ratio of Cho normalized with contralateral Cho was consistently elevated in all primary or metastatic lesions and lower in radiation necrosis. The false elevation of Cho/NAA in non neoplastic conditions can be accounted for by the depression in NAA values with/ without preserved Cho levels. Hence the sensitivity of Cho/NAA for tumor identification is lower compared to the Cho/contralateral Cho. Lactate was seen in 11 lesions and lipids in 9 of the high grade gliomas.

B. Grading of solid intraaxial gliomas

Gliomas are the most common primary brain tumors, varying from very low to a significantly high grade.[15,16] Astrocytomas being the most common subtype. Tumor grade affects treatment planning, response to therapy, prognosis and aggressiveness of followup. So far degree of contrast enhancement, was considered to be directly proportional to the tumor grade. However the presence of contrast enhancement only represents a pathological alteration in the BBB (with or without concomitant angiogenesis). A high grade tumor may have an intact blood brain barrier and fail to enhance or a low grade glioma may have abnormal permeability leading to intense enhancement. On the contrary rCBV[17,18] has been shown to have statistically strong correlation with astrocytoma grading. Even in the study on non-enhancing gliomas statistically significant differences were seen in rCBV ratios between high grade and low grade gliomas.

In our study only 60% of primary intraaxial tumors could be correctly graded using enhancement as an index. One HGG showed low/no enhancement. However rCBV measurements correctly graded all the gliomas suggesting the much stronger relationship between rCBV and tumor grade/survival than the degree of contrast enhancement. There was a statistically significant difference in rCBV ratios between low- and high-grade gliomas (p =0.001) using rCBV of 1.75 as threshold value. Sensitivity and specificity using this cut off value were 100% and 69%, respectively which is in concordance with the findings of Meng Law et al.[19] The HGG without enhancement would have been incorrectly graded on the post contrast T1WI however the rCBV and metabolite parameters were characteristic of a high grade glioma suggesting the superior sensitivity of perfusion MRI in tumor grading. The tumor grades based on rCBV in all the subjects correlated with their histopathologic grade. Most significantly no lesion with exclusively low rCBV proved to be high grade hence no false negatives.

Metabolic parameters[17,20,21] also served as indices of tumor grade. Choline is expected to increase linearly[8,9,10] in solid tumors. We used a threshold value of 1.7 for N-Cho and 1.5 for Cho/NAA and compared the results of Meng Law et al[15] and Cha et al with ours. Low grade gliomas (gradeII) showed (table 2) elevated N-Cho & Cho/NA, low NAA & creatine. Lactate was seen in 2 patients and lipids were not detected in any of the cases. A Myoinositol peak which is expected to be higher in low grade gliomas[24] was seen in 1 case.

High grade gliomas (Grade III - IV)

N-Cho > 1.9 ±0.85, Cr 0.69 ±0.301,cho/NAA 5.1 ±0.76, Cho/Cr 3.5 ±2.6 was seen in high grade gliomas. Among the HGG grade III gliomas showed overall higher choline than grade IV because of the presence of necrosis in the latter. Lactate was elevated in both LGGs and HGGs. Hence the role of lactate for glioma grading remains uncertain. Mobile lipid[23] is present almost exclusively in HGG particularly in GBM, but rarely in LGG. In our study, 6 of the HGG gliomas and none of the LGGs showed significant lipid peaks, suggesting a high specificity although the sensitivity is lower than the lactate peak. Hence our conclusion was grade III gliomas have high rCBV values, very high choline, Cho/NAA & elevated lactate (fig 1) whereas grade IV gliomas are highly perfused with elevated Cho, Cho/NAA (but relatively less than grade IIIs), lactate and more importantly lipid peak (fig 2)

C. Necrotic rim enhancing high grade tumor

Distinction of these from necrotic lesions like abscesses and metastasis can be difficult on conventional MRI although diffusion restriction in abscesses is an important feature. Tumors have a much higher rCBV[22] (mean 1.40, range 1.03-2.20) than abscesses (mean 0.82, range 0.61-0.95). Both cystic tumors and abscesses show increased lactate.[23,24] However abscesses show elevation of acetate, succinate, and some amino acids, as well as lactate. 2 of our patients presented with a rim enhancing necrotic mass and the neuroimaging features were similar to that of a brain abscess. However rCBV was markedly elevated with a mean of 7.2 ±1.6. Elevated choline, and lipid and lactate was suggestive of a high grade tumor like a grade IV glioma (fig 3). Post op histopathology

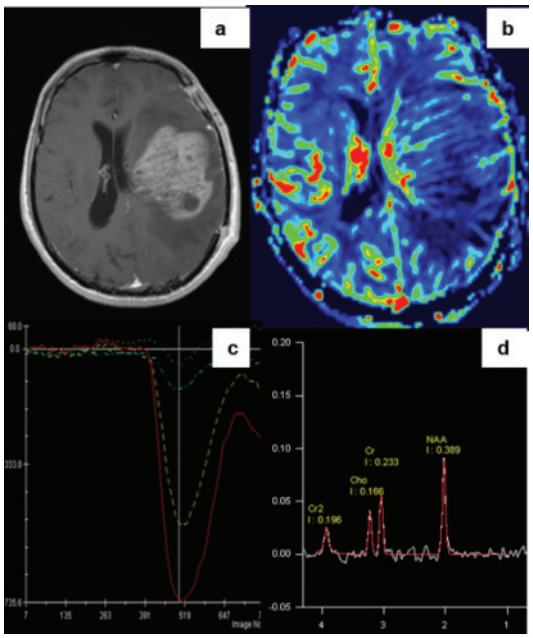

Figure-1: Left frontoparieto temporal lesion grade III anaplastic astrocytoma, showing diffuse enhancement fig (a), moderately elevated perfusion fig (b) and markedly elevated choline fig(d) inverted lactate doublet peak seen at 1.2ppm (arrow)

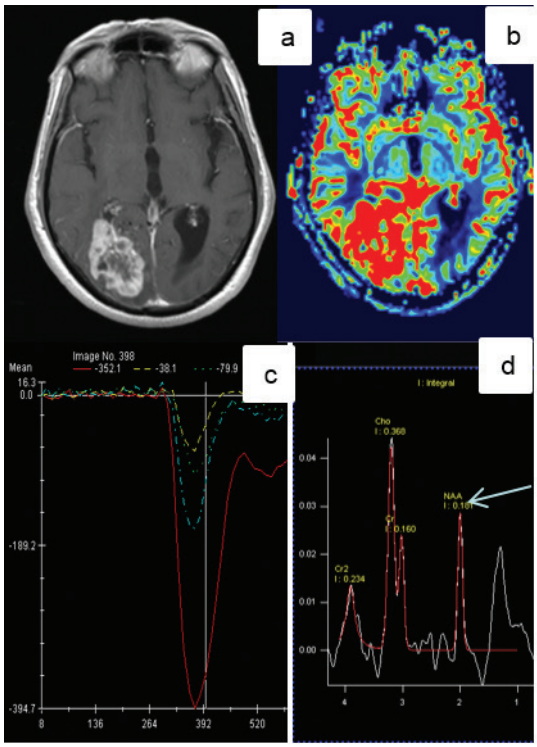

Figure-2: Left occipital GBM fig (a), enhancing fig (b), with very high perfusion fig (c)), significant drop as well as recovery of the time signal intensity curve through the lesion –red curve, moderately elevated choline and upright lipid peak at TE 135 (arrow)

confirmed both the lesions to be GBMs.

C. Nonastrocytic Gliomas

Oligodendrogliomas[25] are well known for their delicate neoangiogenic vessels with elevated rCBV, even in low-grade

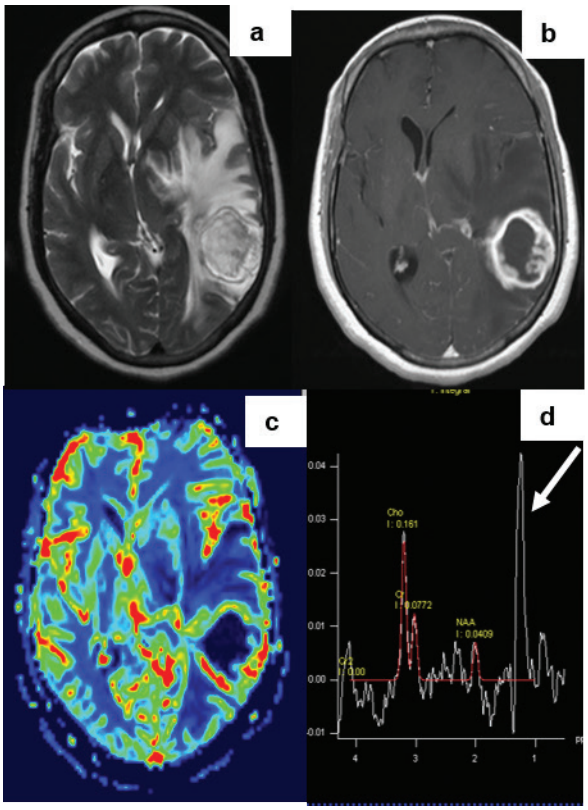

Figure-3: Necrotic Glioblastoma fig (a,b) with very high perfusion through the wall fig (c) elevated choline and lipids-(arrow) fig (d). No amino acid peaks seen at TE 135

tumors, that can be as high as that of Glioblastoma.[20] However cortical involvement, frontal lobe predominance, intratumoral cysts and susceptibility changes due to intratumoral calcification in conjunction with high rCBV, can help in preoperative diagnosis. The oligodendrogliomas (2) in our study demonstrated high perfusion mean rCBV values 5.7 ±0.8. Mean N-Cho 2.7 ±1.4, NAA 0.2 ±.1, creatine 0.8 ±0.2, Cho/NAA 2.8 ±0.14, Cho/Cr 1.2 ± 0.4 correlated with results of previous studies.[20]

D. Metastatic brain tumors

Approximately 30% brain metastasis,[26] can manifest as a single lesion or can be the initial clinical presentation of systemic malignancy. These may be difficult to differentiate from solid HGG. However the quantitative analysis of T2* relaxivity signal intensity time curve characteristics i.e. (peak height and percentage of signal intensity recovery) can be used to differentiate GBM and single brain metastasis.[26] Lack of BBB in metastasis leads to profound contrast leakage in the early bolus phase. We found more than 82% signal intensity recovery in GBM and less than 66%, in brain metastasis. Volume of tumor showing less than 50% signal intensity recovery during the recirculation phase was much greater in brain metastasis than in GBM (fig 4). Also GBMs had more peak height due to higher tumor angiogenesis than brain metastasis. The average peak height in the non enhancing PTL was significantly higher in GBM {1.31 ± 0.97 (mean ± SD)} than in brain metastasis0.39 ± 0.19. The

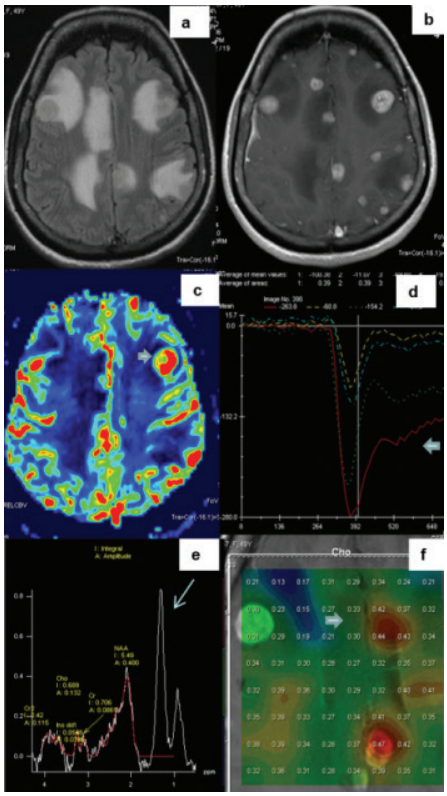

Figure-4: Metastasis from Bronchogenic Carcinoma. Multiple focal fig (a) enhancing lesions fig (b), showing very high perfusion fig (c), Mean curves fig (d) show partial recovery of the time signal intensity curve (arrow) secondary to contrast extravasation due to an absent BBB. and high choline fig (d) and elevated lipids (arrow). Choline and rCBV appearing normal in the peritumoral region (arrow head)

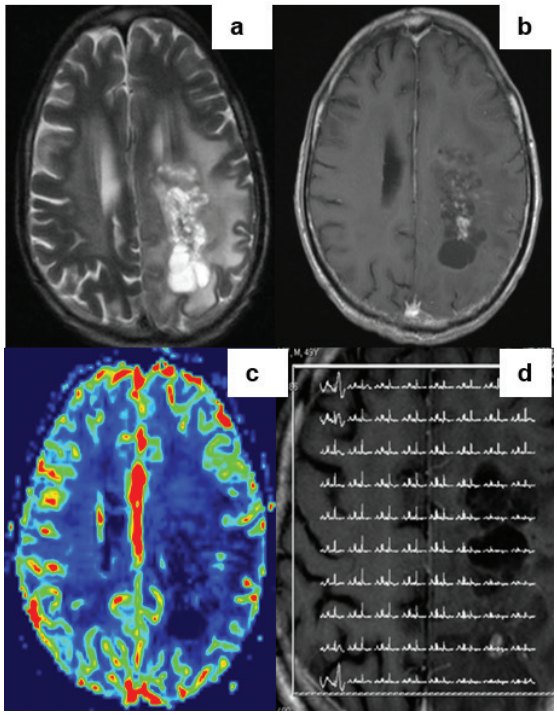

Figure-5: Left parietal operative site fig (a) showing enhancing soft tissue fig (b) Low perfusion fig (c) and absent metabolites fig (d) s/o post radiotherapy necrosis

difference was statistically significant (P <.001). Metastasis showed high choline and Cho/NAA, low creatine, absent or very low NAA- and a strong lipid peak with no pathologic spectra outside the region of enhancement (fig 4). Cho/Cr ratio was 2.28 ± 1.24 in the peritumoral region of gliomas but 0.76 ± 0.23 in metastases. The difference was statistically significant (P =.001).

E. Radiation Necrosis vs. Recurrent Tumor: Radiation necrosis as well as radiation induced demyelination commonly presents as an enhancing mass with variable edema and mass effect making it impossible to differentiate it from tumor recurrence. Additionally these lesions occur within 2 yrs after radiation, the same time period during which tumor recurrence is most frequent.

We evaluated eight cases of previously treated gliomas. All lesions showed nonspecific contrast enhancement. Seven lesions showed elevated rCBV, Cho, Cho/NAA, Cho/Cr and depressed NAA suggestive of residual or recurrent lesions. One enhancing lesion showed rCBV values lower than the contralateral white matter and flattened peaks with depressed NAA, Cho, and Cr. An intense peak consistent with lactate and lipids was seen between 0.9 – 1.5ppm at TE 135 –, indicative of cellular break down products seen in radiation necrosis (fig 5). Our findings were consistent with those of Roland G Henry et al[28] and A.Aria Tzika et al.[29]

CONCLUSION

Perfusion MRI and spectroscopy allowed preoperative identification and grading of brain tumors, characterization as primary intraaxial or metasttic tumor as well as distinction of viable tumor tissue from post treatment changes.

ABBREVIATIONS

N-Cho	Normalized choline
N-NAA	Normalized N-acetyl aspartate
N-Cr	Normalized creatine
GBM	Glioblastoma multiformae
HGG	high grade glioma
LGG	low grade glioma

REFERENCES

1. Thomas Hacklander, Jurgen R. Reichenbach, Matthias Hofer, and Ulrich Modder. Measurement of cerebral blood volume via the relaxing effect of low-dose gadopentetate dimeglumine during bolus transit AJNR 1996;517:821–830.
2. Alan Jackson, et al. Abnormalities in the recirculation phase ofcontrast agent bolus passage in cerebral gliomas: comparison with relative blood volume AJNR 2002 ;23:7–14.
3. Jeffrey R. Petrella and James M. Provenzale. MR perfusion imaging of the brain techniques and applications *AJR* 2000;175:207-219

4. Kathleen M. Schmainda et al. Characterization of a first-pass gradient-echo spin-echo method to predict brain tumor grade and angiogenesis.AJNR 2004;25:1524-1532.
5. Jimmie C. Wong, James M. Provenzale and Jeffrey R. Petrella Perfusion MR imaging of brain neoplasms.Department of radiology, Duke University medical center, box 3808, Durham, nc 27710
6. Dorothee Ott Hennig, Ernst. Human brain tumors: assessment with in vivo proton mr spectroscopy' Radiology 1993; 186:745-752
7. Michael J. Fuiham, J. Dietz, ShihRamesh Raman, S. Sobering. Mapping of Brain tumor metabolites with proton MR spectroscopic imaging: clinical relevance' Radiology 1992; 185:675-686
8. Michael J. Fuiham Bizzi, J. Dietz, Ramesh Raman. Mapping ofBrain Tumor metabolites with proton MR spectroscopic imaging: clinical relevance' Radiology 1992; 185:675-686
9. Sarah J. Nelson Multivoxel Magnetic Resonance Spectroscopy of Brain Tumors *Vol. 2, 497-507, May 2003* Molecular Cancer Therapeutics
10. Mauricio Castillo, Lester Kwock, and Suresh K. Mukherji. Clinical applications of proton MR spectroscopy AJNR 1996 ;17:1–15.
11. Harald Kugel, Heindel, Human Brain Tumors: Spectral Patterns Detected with Localized H1MR spectroscopy Radiology 1992; 183:701-709
12. Mauricio Castillo, Lester Kwock, and Suresh K. Mukherji. Clinical applications of proton MR spectroscopy AJNR 1996;17:1–15.
13. Harald Kugel, Heindel, Human Brain Tumors: Spectral Patterns Detected with Localized H1MR spectroscopy Radiology 1992; 183:701-709
14. Nail Bulakbasi, Murat, Fatih, Cem and Taner Uçoz. Combination of single-voxel proton MR spectroscopy and apparent diffusion coefficient calculation in the evaluation of common brain tumors AJNR 2003;24:225-233.
15. Meng Law, MD, Sarah Oh, MD, James S. Babb, PhD, Edwin Wang, MD, Matilde. Low-grade gliomas: dynamic susceptibility-weighted contrast-enhanced perfusion MR imaging—prediction of patient clinical response *Radiology* 2006;238:658-667
16. Ji Hoon Shin, Ho Kyu, Byung Duk, Jin-Suh, Weechang. Using relative cerebral blood flow and volume to evaluate the histopathologic grade of cerebral gliomas: preliminary results. *AJR* 2002; 179:783-789
17. Xiaojuan Li, Daniel B et al. Relationship of MR-derived lactate, mobile lipids, and relative blood volume for gliomas in vivo AJNR 2005;26:760-769.
18. Anup H. Parikh,J. Keith Smith, Matthew G. Ewend, Elizabeth Bullitt. Correlation of MR perfusion imaging and vessel tortuosity parameters in assessment of intracranial neoplasms technology in cancer research & treatment 2004;10:1533-0346.
19. Meng Law, Stanley, James S. Babb, Edmond A. Knopp, John G. Golfinos, David Zagzag and Glyn Johnson. Comparison of cerebral blood volume and vascular permeability from dynamic susceptibility contrast-enhanced perfusion MR imaging with glioma grade AJNR 2004;5:746-755.
20. Loukas G. Astrakas et al.Noninvasive magnetic resonance spectroscopic imaging biomarkers to predict the clinical grade of pediatric brain tumors Cancer Research Vol. 10, 8220-8228, December 15, 2004
21. J.M. Lupo S. ChaS.M. Chang S.J. Nelson.Analysis of metabolic indices in regions of abnormal perfusion in patients with high-grade glioma AJNR Am J Neuroradiol 28:1455– 61 Sep 2007 13
22. James Provenzale, Srinivas Mukundan and Danial.P.barboriak. Diffusion weighted and perfusion imaging for brain tumor characterization & assessment of treatment response. Radiology 2006; 239: 632-649.
23. Ping H., Jih T. L. Huay B. and Chien F. Yang. Brain abscess and necrotic brain tumor: discrimination with proton MR spectroscopy and diffusion-weighted imaging AJNR 23:1369-1377, September 2002
24. Nail Bulakbasi, Murat Kocaoglu, Anar Farzaliyev, Cem Tayfun, Taner Ucoz and Ibrahim Somuncu. Assessment of Diagnostic Accuracy of Perfusion MR Imaging in Primary and Metastatic Solitary Malignant Brain Tumors AJNR 26:2187-2199, October 2005
25. M. Vittoria Spampinato Lester Kwock1 Matthew Ewend John D. Grimme Daniel L. A. Camacho. Cerebral blood volume measurements and proton mr spectroscopy in grading of oligodendroglial tumors AJR 2007; 188:204–212
26. S. Cha,Lupo M.-H. Chen K.R. Lamborn M.W. McDermott Cha. Differentiation of glioblastoma multiforme and single brain metastasis by peak height and percentage of signal intensity recovery derived from dynamic susceptibility-weighted contrast- enhanced perfusion MR Imaging AJNR 2007;28:6-20
27. Benjamin A. Cohen Edmond A. Knopp, Henry Rusinek, Songtao and Oded Brain compression without global neuronal loss in meningiomas: whole-brain proton MR spectroscopy report AJNR 26:2178-2182, October 2005
28. Roland G. Henry, Daniel B. Vigneron, Nancy J., P. Ellen, Mark R., Susan M., Joshua M. Star-, Lawrence L., William P., Susan M. and Sarah J. Comparison of relative cerebral blood volume and proton spectroscopy in patients with treated gliomas AJNR 2000;21:357-366
29. Aria Tzika, Sridhar Vajapeyam, and Patrick D. Barnes Multivoxel Proton mr spectroscopy and hemodynamic MR imaging of childhood brain tumors: preliminary observations. AJNR Am J Neuroradiol 1997;18:203–218.
30. Yair Safriel, Gordon, Kaye and Joachim Baehring MR Spectroscopy in the diagnosis of cerebral amyloid angiopathy presenting as a brain tumor AJNR 25:1705-1708.